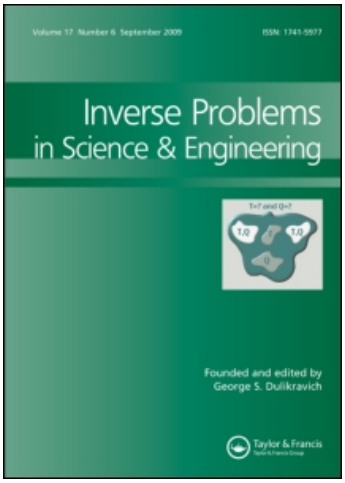

Inverse Problems in Science and Engineering
Publication details, including instructions for authors and subscription information:
http://www.informaworld.com/smpp/title~content=t713643452

An improved quantum-behaved particle swarm optimization with perturbation operator and its application in estimating groundwater contaminant source

Na Tian[ab]; Jun Sun[a]; Wenbo Xu[a]; Choi-Hong Lai[b]
[a] School of Information Technology, Jiangnan University, Wuxi 214122, China [b] School of Computing and Mathematical Science, University of Greenwich, London SE10 9LS, UK

Online publication date: 14 March 2011

To cite this Article Tian, Na , Sun, Jun , Xu, Wenbo and Lai, Choi-Hong(2011) 'An improved quantum-behaved particle swarm optimization with perturbation operator and its application in estimating groundwater contaminant source', Inverse Problems in Science and Engineering, 19: 2, 181 — 202
To link to this Article: DOI: 10.1080/17415977.2010.531470
URL: http://dx.doi.org/10.1080/17415977.2010.531470

Inverse Problems in Science and Engineering
Vol. 19, No. 2, March 2011, 181–202

Taylor & Francis
Taylor & Francis Group

An improved quantum-behaved particle swarm optimization with perturbation operator and its application in estimating groundwater contaminant source

Na Tian[ab]*, Jun Sun[a], Wenbo Xu[a] and Choi-Hong Lai[b]

[a]*School of Information Technology, Jiangnan University, Wuxi 214122, China;*
[b]*School of Computing and Mathematical Science, University of Greenwich, London SE10 9LS, UK*

(*Received 16 May 2010; final version received 6 October 2010*)

In this study, a heuristic method known as quantum-behaved particle swarm optimization (QPSO) is used to solve the inverse advection–dispersion problem of estimating the strength of a time-varying groundwater contaminant source from the knowledge of forensic observations. No prior information of the functional form is given in this study. The implicit upwind finite difference method is used in the governing advection–dispersion equation. The least squares method is used to model the inverse problem, which transforms to an optimization problem. Considering the ill-posedness of the inverse problem, the Tikhonov regularization method is used to stablize the inverse solution. To ensure the global convergence properties of the QPSO, an improved version with the perturbation operator is proposed and its performance is tested by several well-known benchmark functions. Finally, the proposed method is applied to reconstruct the contaminant source history and comparisons with other methods are also presented in this article. The numerical experiments demonstrate the efficiency and validity of our proposed method.

Keywords: quantum-behaved particle swarm optimization; groundwater contaminant source identification; inverse problem; advection–dispersion; Tikhonov regularization; perturbation operator

1. Introduction

Environmental contamination is a widespread problem that may affect the utility of an environmental resource, such as a groundwater aquifer or a surface water body. Identifying contaminant sources in groundwater is important for developing effective remediation strategies and identifying responsible parties in a contamination incident. Groundwater contamination broadly defines any constituent that reduces the quality of groundwater. Contamination can be chemical, physical or biological. Chemical contamination can be broken down further into soluble components and non-aqueous phase liquid components. Soluble components are dissolved in groundwater and are transported with the groundwater as it moves. Non-aqueous phase liquids are bodies of liquid that are

*Corresponding author. Email: tn24@gre.ac.uk

ISSN 1741–5977 print/ISSN 1741–5985 online

DOI: 10.1080/17415977.2010.531470
http://www.informaworld.com

separate from the water and are generally not transported with bulk groundwater movement. This study addresses the transport of dissolved chemicals in water-saturated porous media. Transport of soluble chemicals is subjected to the process of advection and dispersion, the mathematical model is given in Equation (1). Advection describes the movement of a contaminant along with the bulk movement of groundwater. Dispersion describes the spreading of a contaminant as it moves through the porous media.

If the initial and boundary conditions, model parameters and contaminant release history are known, the advection–dispersion equation can be solved directly using analytical techniques or numerical simulations to obtain the distribution of contaminant concentration. This process is called forward advection–dispersion problem, which has a unique solution and is well-posed. In contrast, the inverse advection–dispersion problem for groundwater models considered here involves the determination of the unknown time-dependent contaminant release history from the knowledge of concentration measurements taken within the medium. The inverse problem of groundwater source identification is ill-posed. Because concentration data are sampled at finite discrete points, infinite number of source history functions can produce the measured data; therefore, the solution of this inverse problem is not unique. In addition, the solution of the inverse problem is very sensitive to the unavoidable measurement noise and computing error, which is known as instability.

In this article, we study a source history reconstruction problem, with a point source of contamination at a known location in a one-dimensional flow field. The spatial distribution of the contaminant concentration is sampled at a specific time after the initial source release, which is used with inverse methods to reconstruct the time-varying contaminant source history.

During the past decade, inverse problems of groundwater contaminant transport have received wide attention. A concise review of the most relevant work is given in Ref. [1]. Gorelick *et al*. [2] used the least squares and linear programming to determine the location and strength of the source pollutant in the field. Their numerical model was tested on two sets of hypothetical data representing a steady-state case and a transient case. The model assumed other transport parameters, which are previously known. Wagner [3] estimated the transport parameters and contaminant source simultaneously. Zou and Parr [4] developed an analytical solution to determine the longitudinal and transverse dispersivities. Skaggs and Kabala [5–7] solved the inverse source problem with Tikhonov regularization and the method of quasi-reversibility. Woodbury and Ulrych [8,9] solved the problem using minimum relative entropy (MRE) inversion. Snodgrass and Kitanidis [10] used a geostatistical approach to solve the same problem. In Refs [11–15], some optimization methods, such as conjugate gradient method, are used to solve various inverse problems, as they converge fast but strongly depend on initial guess and cannot guarantee the global optimum. The Tikhonov regularization method is more robust in solving the inverse problem with noisy sampling; however, it cannot reconstruct the non-smooth source history efficiently. The MRE method is a gradient-based approach, which is more efficient in dealing with the source history with many peaks. But it is not effective for problems that contain a measurement error of unknown magnitude. Furthermore, the gradient computation of the objective function is very complicated, and the gradient may even not exist for some objective functions. The determination of the Lagrange multiplier is also a key difficulty in the MRE method.

For these types of problems, heuristic global search approaches, such as particle swarm optimization (PSO) are more effective, Bharat *et al.* [16] first use PSO to solve the inverse source problem, but PSO is not robust enough to stabilize the inverse solution.

In this study, another swarm intelligence method named as quantum-behaved particle swarm optimization (QPSO) is presented to reconstruct the contaminant source history. QPSO, inspired by quantum mechanics, was proposed by Sun [17–19] from the knowledge of PSO. PSO was originally proposed by Kennedy and Eberhart [20] as a simulation of social behaviour, such as fish schooling and bird flocking. QPSO can be easily implemented and is computationally inexpensive, since its memory and CPU speed requirements are low. Moreover, it does not require gradient information of the objective function under consideration, but only its values, and it uses only primitive mathematical operators. Compared with PSO, QPSO has fewer parameters to set and has only position to iterate but no velocity. In order to enhance the global search ability of QPSO, an improved version with a perturbation operator is proposed in this article. The numerical experimental results demonstrate the validity and efficiency of the proposed method to solve the inverse source history problems. Comparison with other stochastic methods is also presented in this study.

The rest of this article is organized as follows. In Section 2, the mathematical model of the inverse source history problem is described. Section 3 describes the PSO and QPSO in detail, the description of improved QPSO with perturbation operator is also given in this section. The benchmark tests of the proposed method are presented in Section 4. In Section 5, the improved QPSO is applied to the inverse source history problems. Finally, Section 6 gives the conclusion.

2. Mathematical model of inverse source problems

In general, the governing equation for contaminant transport in groundwater is the advection–dispersion equation, which, for a one-dimensional contaminant solute transport through a saturated homogeneous porous medium, is:

$$\frac{\partial C(x,t)}{\partial t} = D\frac{\partial^2 C(x,t)}{\partial x^2} - V\frac{\partial C(x,t)}{\partial x}, \quad 0 < x < L, \quad t > 0, \tag{1}$$

$$C(x,0) = C_0(x), \quad 0 \le x \le L, \tag{2}$$

$$C(0,t) = C_{in}(t), \quad t \ge 0, \tag{3}$$

$$C(L,t) = 0, \quad t \ge 0, \tag{4}$$

where $C(x, t)$ is the contaminant concentration at a spatial location x and time t, D is a constant dispersion coefficient, V is a uniform steady pore velocity, $C_{in}(t)$ is the source history for a source located at $x = 0$ and $C_0(x)$ is the initial spatial distribution of the contaminant concentration. The first term on the right-hand side of Equation (1) is the dispersion term and the second term is advection term.

Measurements of contaminant concentration are available at N discrete locations $Y(x_i, t)$(where x_i is the ith sampling location, $i = 1, \ldots, N$). In the literature, three types of samples are included: samples taken at one location over a period of time, samples taken at

many locations at one time or a combination of the two. Comparison of the results obtained by different types of samples will be presented in Section 5.

We want to find such a source, with which the concentration $C(x_i, t)$ computed from Equations (1)–(4) is as close to the measured concentration $Y(x_i, t)$ as possible, so the following equation is modelled by the least squares method:

$$\min J[C_{in}(t)] = \int_{t=0}^{t_f} \sum_{i=1}^{N} (C(x_i, t) - Y(x_i, t))^2 \, \mathrm{d}t. \tag{5}$$

Then the inverse source problem is cast as an optimization problem, which intends to minimize Equation (5).

For the forward advection–dispersion problem, analytical techniques or numerical simulation can be used to obtain the solution $C(x, t)$. But there are many limitations for the analytical techniques if the boundary or initial conditions, dispersion, or flow velocity are nonlinear, while the numerical methods, such as finite difference method, finite volume method and finite element method, may be suitable for all types of functional forms of the equation. In this study, the implicit upwind finite difference method is used to discretize Equation (1), which is shown in Equation (6), because of the advection term of Equation (1), the central difference will easily lead to oscillation in the solution:

$$\frac{C_i^{j+1} - C_i^j}{\Delta t} = D \frac{C_{i+1}^{j+1} - 2C_i^{j+1} + C_{i-1}^{j+1}}{\Delta x^2} - V \frac{C_{i+1}^{j+1} - C_i^{j+1}}{\Delta x}, \tag{6}$$

where C_i^j is the concentration at the j time step, i mesh step ($i = 1, 2, \ldots, N_x$, N_x is the number of spatial grid; $j = 1, 2, \ldots, , N_t$, N_t is the number of time steps), Δt is the time incremental size and Δx is the mesh size.

The average error of the estimated source history may be defined as

$$\text{average\_error} = \frac{1}{N_t} \sqrt{\sum_{j=1}^{N_t} [\overline{C_{in}}(t_j) - C_{in}(t_j)]^2}, \tag{7}$$

where $\overline{C_{in}}(t)$ is the estimated source history and $C_{in}(t)$ is the exact source.

This inverse problem is ill-posed, the unavoidable measurement noise and numerical computing errors often lead to unstable or inaccurate results. Therefore, a regularization technique have to be adopted to stabilize the solution, here the Tikhonov regularization method [21] is used, which change the objective function to a well-posed

$$\min J[C_{in}(t)] = \int_{t=0}^{t_f} \sum_{i=1}^{N} (C(x_i, t) - Y(x_i, t))^2 \, \mathrm{d}t + \lambda^2 \left\| LC_{in}(t) \right\|^2, \tag{8}$$

where λ is the regularization parameter, the first term and the second term on the right-hand side of Equation (8) is the discrepancy term and the regularization term, respectively. The regularization operator is generally of the form

$$\left\| LC_{in}(t) \right\|^2 = \int_0^{t_f} \left(\frac{\mathrm{d}^n C_{in}(t)}{\mathrm{d}t^n} \right)^2 \mathrm{d}t. \tag{9}$$

The zeroth- and first-order regularization terms are commonly used.

If $n=0$, zeroth-order regularization term is used, which minimizes the norm of the input function:

$$\min J[C_{in}(t)] = \int_{t=0}^{t_f} \sum_{i=1}^{N} (C(x_i,t) - Y(x_i,t))^2 \,\mathrm{d}t + \lambda^2 \int_{t=0}^{t_f} (C_{in}(t))^2 \,\mathrm{d}t. \tag{10}$$

If $n=1$, first-order regularization is used, which minimizes the oscillatory nature of the input function:

$$\min J[C_{in}(t)] = \int_{t=0}^{t_f} \sum_{i=1}^{N} (C(x_i,t) - Y(x_i,t))^2 \,\mathrm{d}t + \lambda^2 \int_{t=0}^{t_f} \left(\frac{\mathrm{d}C_{in}(t)}{\mathrm{d}t}\right)^2 \mathrm{d}t. \tag{11}$$

The regularization stabilizes the solution, minimization of $J[C_{in}(t)]$ in Equation (8) is a trade-off between the matching data, and stabilizing solution. The values chosen for λ influence the stability of the solution. As $\lambda \to 0$, the solution exhibits oscillatory behaviour and becomes unstable. On the other hand, with large values of λ, the solution is damped and deviates from the exact result. Tikhonov suggested that λ should be selected according to the discrepancy principle – the minimum value of the objective function is equal to the sum of the squares of the errors due to the measurements. It is also possible to use the L-curve method [22,23] to find the best value of λ, in which the regularization term $\left\|LC_{in}(t)\right\|^2$ is plotted on a log–log plot against the residual term $\int_{t=0}^{t_f} \sum_{i=1}^{N} (C(x_i,t) - Y(x_i,t))^2 \,\mathrm{d}t$ for many values of the regularization parameter λ. The value of the regularization parameter at the corner of the L-curve is the optimal parameter value. This method illustrates the trade-off between minimizing the residual and minimizing the regularization.

3. An Improved QPSO with a perturbation operator

3.1. *Particle swarm optimization*

PSO algorithm is a population-based optimization technique originally introduced by Kennedy and Eberhart in 1995 [20]. A PSO system simulates the knowledge evolvement of a social organism, in which individuals (particles) representing the candidate solutions of an optimization problem traverse through a multidimensional search space in order to allow the optima or sub-optima to be determined. The position of each particle is evaluated according to a goal (objective function) at every iteration, and particles in a local neighbourhood share memories of their 'best' positions. These memories are used to adjust the particles' own velocities, and their subsequent positions. It has already been shown that the PSO algorithm is comparable in performance with and may be considered as an alternative to the genetic algorithm (GA) [24].

In PSO system with M particles, each individual is treated as a volume-less particle in the D-dimensional space, with the position vector and velocity vector of particle i at the kth iteration represented as $X_i(k) = (X_{i1}(k), X_{i2}(k), \ldots, X_{iD}(k))$ and $V_i(k) = (V_{i1}(k), V_{i2}(k), \ldots, V_{iD}(k))$.

There are different versions of PSO algorithm proposed by various researchers to improve the performance of the algorithm since it was first proposed in 1995. The most important improvements are the version with the inertia weight ω [25] and the one with

constriction factor χ [26]. In inertia weight PSO, the velocity is updated by

$$V_i(k+1) = \omega \cdot V_i(k) + c_1 \cdot r_1 \cdot (P_i - X_i(k)) + c_2 \cdot r_2 \cdot (P_g - X_i(k)), \tag{12}$$

$$\omega = (\omega_0 - \omega_1) \times (k_{\max} - k)/k_{\max} + \omega_1, \tag{13}$$

while in the constriction factor model, the velocity is manipulated by

$$V_i(k+1) = \chi \cdot [V_i(k) + c_1 \cdot r_2 \cdot (P_i(k) - X_i(k)) + c_2 \cdot r_2 \cdot (P_g - X_i(k))], \tag{14}$$

where

$$\chi = \frac{2}{\left|2 - \phi - \sqrt{\phi^2 - 4\phi}\right|}, \quad \phi = c_1 + c_2, \quad \phi > 4. \tag{15}$$

Then the particle moves according to the following equation:

$$X_i(k+1) = X_i(k) + V_i(k+1), \tag{16}$$

where $i = 1, 2, \ldots, M$, ω is the inertia weight, which may decrease linearly according to the generation, c_1 and c_2 are the acceleration coefficients, r_1 and r_2 are the random numbers uniformly distributed in $(0, 1)$, $P_i = (P_{i1}, P_{i2}, \ldots, P_{iD})$ is the best previous position (the position giving the best objective function value) of particle i which is known as the personal best position and $P_g = (P_{g1}, P_{g2}, \ldots, P_{gD})$ is the position of the best particle among all the particles in the population which is known as the global best position. In this article, PSO with inertia weight (PSO-IW) is used to solve the inverse source history problem, in which every particle $X_i(k)$ is treated as a candidate solution of the unknown source function $C_{in}(t)$.

$$\begin{aligned} X_i(k) &= \{X_{i1}(k), X_{i2}(k), \ldots, X_{iD}(k)\} \\ &= \{C_{in}(t_1), C_{in}(t_2), \ldots, C_{in}(t_{N_t})\}. \end{aligned} \tag{17}$$

Here the dimension D is equal to the number of time steps N_t. Equation (8) is used as the objective function to evaluate the particles.

3.1.1. *Procedure of PSO-IW for this inverse source problem*

Initialize particles with random positions and velocities:

$$X(0) = \{X_1(0), X_2(0), \ldots, X_i(0), \ldots, X_M(0)\};$$
$$V(0) = \{V_1(0), V_2(0), \ldots, V_i(0), \ldots, V_M(0)\};$$

Initialize *pbest* P, *gbest* P_g, inertia weight ω and acceleration coefficient c_1, c_2, $k = 0$, stopping criteria ε;

While ($k < k_{\max}$) or (ε is not reached)
  Update position of all particles according to Equation (16);
  Update velocity of all particles according to Equation (12);
  Apply velocity limits $V_{\max}$ to velocities;
  Evaluate all the particles $J[X_i(k)]$, $i = 1, 2, \ldots, M$ according to Equation (8);
  Update *pbest* P and *gbest* P_g;
  Update inertia weight ω according to Equation (13);
  $k = k + 1$;
End while
Output *gbest* P_g.

3.2. *Quantum-behaved particle swarm optimization*

The main disadvantage of the original PSO algorithm is that it is not guaranteed to be global convergent [27]. The concept of a QPSO was developed to address the disadvantage and first reported at conferences, such as in Refs [17–19]. Trajectory analysis in Ref. [28] demonstrated the fact that the convergence of the PSO algorithm may be achieved if each particle converges to its local attractor, $p_i = (p_{i1}, p_{i2}, \ldots, p_{iD})$ is defined at the coordinate

$$p_i(k) = \varphi \cdot P_i(k) + (1 - \varphi) \cdot P_g(k), \tag{18}$$

where P_i is the personal best position of particle i and P_g is the global best position of all particles, $\varphi \in (0, 1)$. It can be seen that p_i is a stochastic attractor of particle i that lies in a hyper-rectangle with P_i and P_g being two ends of its diagonal and moves following P_i and P_g. In fact, when the particles are converging to their own local attractors, their personal best positions, local attractors and the global best positions will all converge to one point, leading the PSO algorithm to converge.

The particle moves around and careens towards point p_i with its kinetic energy (velocity) declining to zero, like a returning satellite orbiting the earth. From the point view of dynamics, to avoid explosion and to guarantee convergence, the particle must be in bound state, move in an attraction potential field whose centre is point p_i. In terms of classical dynamics, the particle in the original PSO system must fly in an attraction potential field to guarantee its bound state. Correspondingly, it is also indispensable for the particles of PSO with quantum behaviour to move in a potential field that can ensure bound state of the particle. In QPSO, δ potential well is employed to bind the particle for the sake of convergence. The philosophy of the QPSO is formulated as follows.

We assume that the PSO system is a quantum system, with each particle in a quantum state formulated by wave function ψ. $|\psi|^2$ is the probability density function of the position of the particle. Inspired by the analysis of convergence of the traditional PSO in Ref. [28], we further assume that, at iteration k, particle i moves in D-dimensional space with a δ potential well at $p_i(k)$. Correspondingly, the wave function at iteration $k+1$ is

$$\psi(X_i(k+1)) = \frac{1}{\sqrt{L_i(k)}} \exp\left(-\frac{|X_i(k+1) - p_i(k)|}{L_i(k)}\right). \tag{19}$$

Hence, the probability density function Q is a double exponential distribution as follows:

$$Q(X_i(k+1)) = |\psi(X_i(k+1))|^2 = \frac{1}{L_i(k)} \exp\left(-2 \cdot \frac{|X_i(k+1)| - p_i(k)}{L_i(k)}\right) \tag{20}$$

and thus the probability distribution function F is

$$F(X_i(k+1)) = \exp\left(-2 \cdot \frac{|X_i(k+1) - p_i(k)|}{L_i(k)}\right), \tag{21}$$

where $L_i(k)$ is the standard deviation of the double exponential distribution. Using the Monte Carlo method, we can obtain the position X_i at iteration $k+1$ as

$$X_i(k+1) = p_i(k) \pm \frac{L_i(k)}{2} \ln\left(\frac{1}{u}\right), \quad u \sim U(0, 1), \tag{22}$$

where u is a random number uniformly distributed in (0, 1), $L_i(k)$ is evaluated by

$$L_i(k) = 2 \cdot \alpha \cdot \left|C(k) - X_i(k)\right|, \tag{23}$$

where C, called mean best position, is defined as the mean of the *pbest* positions of all particles. That is

$$C(k) = (C_1(k), C_2(k), \ldots, C_D(k)) = \left(\frac{1}{M}\sum_{i=1}^{M} P_{i1}(k), \frac{1}{M}\sum_{i=1}^{M} P_{i2}(k), \ldots, \frac{1}{M}\sum_{i=1}^{M} P_{iD}(k)\right), \tag{24}$$

where M is the population size and P_i is the personal best position of particle i. Hence, the position of the particle updates according to the following equation:

$$X_i(k+1) = p_i(k) \pm \alpha \cdot \left|C_i(k) - X_i(k)\right| \cdot \ln\left(\frac{1}{u}\right). \tag{25}$$

The parameter α in Equation (25) is known as the contraction–expansion coefficient, which can be adjusted to control the speed of convergence, in many cases, good performance may be achieved if α varies linearly from α_0 to α_1 ($\alpha_0 > \alpha_1$) over the iteration in the QPSO method, i.e.

$$\alpha = (\alpha_0 - \alpha_1) \times (k_{\max} - k)/k_{\max} + \alpha_1, \tag{26}$$

where $k_{\max}$ is the maximum number of iterations and k is the current iteration number.

The QPSO method is different from the PSO method in that the iterative update of the former method is given by Equation (25) ensuring particles appear in the entire D-dimensional search space during each of the iteration steps, while the particles in the latter method can only move in a bounded space. Using the global convergence criterion in Ref. [27], one can conclude that the QPSO method is a global convergent algorithm, whereas the original PSO method with Equation (12) or (14) is not. Moreover, unlike the original PSO method, the QPSO method does not require velocity vectors for the particles at all and has fewer parameters to control, making the method easier to implement. Experimental results performed on some well-known benchmark functions show that the QPSO method has better performance than the original PSO method [17–19].

3.2.1. *Procedure of QPSO for inverse source problems*

Initialize particles with random positions

$$X(0) = \{X_1(0), X_2(0), \ldots, X_i(0), \ldots, X_M(0)\};$$

Initialize *pbest* P, *gbest* P_g, contraction–expansion coefficient α, $k = 0$, stopping criteria ε;

While ($k < k_{\max}$) or (ε is not reached)
  Compute the mean best position C by Equation (24);
  Compute p by Equation (18);
  Update the positions of all particles according to Equation (25);
  Evaluate all the particles $J[X_i(k)]$, $i = 1, 2, \ldots, M$ according to Equation (8);
  Update *pbest* P and *gbest* P_g;
  Update contraction–expansion coefficient according to Equation (26);
  $k = k + 1$;
End while
Output *gbest* P_g.

3.3. *An improved QPSO*

The global convergence of QPSO or other random search algorithm means that the algorithm will hit the global optimal solution with infinite number of iterations. However, when the algorithm is applied to the real-world problems, only a finite number of iterations is allowed, so that the premature convergence is inevitable and there is much room for improvement for QPSO, particularly when the algorithm is used to solve the present complex ill-posed problem. So far, many supplication strategies have been proposed to enhance the search ability of the algorithm [29–31]. In this study, we incorporate a novel perturbation operation into the algorithm to enhance the efficiency of QPSO in finding the global optimal solutions on complex functional terrains [32,33]. In this improved version of QPSO, the diversity of the swarm can be enhanced by exerting the random perturbation on each particle as follows:

$$X_i^{per}(k) = X_i(k) + pert_{coff} \times X_i(k) \times (r_1 - r_2), \tag{27}$$

where $pert_{coff} = a \times \exp(2.3025851 \times (k_{\max} - k)/(k_{\max} - 1))$ is a nonlinear perturbation coefficient varying from $10 \times a$ to a (a is a scale parameter which can be adjusted according to the specific problems) shown in Figure 1, and r_1, r_2 are uniformly distributed random numbers in (0,1). This diversification strategy can indeed improve the global search ability of the swarm, particularly at the later stage of search process when the diversity is at such a low level that the further global search is impossible for the particles, consequently leading the algorithm to premature convergence.

3.3.1. *Procedure of improved QPSO (QPSO-PER) for inverse source problems*

Initialize particles with random positions $X(0) = \{X_1(0), X_2(0), \ldots, X_i(0), \ldots, X_M(0)\}$;

Initialize *pbest* P, *gbest* P_g, contraction–expansion coefficient α, $k = 0$, stopping criteria ε;

While ($k < k_{\max}$) or (ε is not reached)

Compute the mean best by Equation (24);

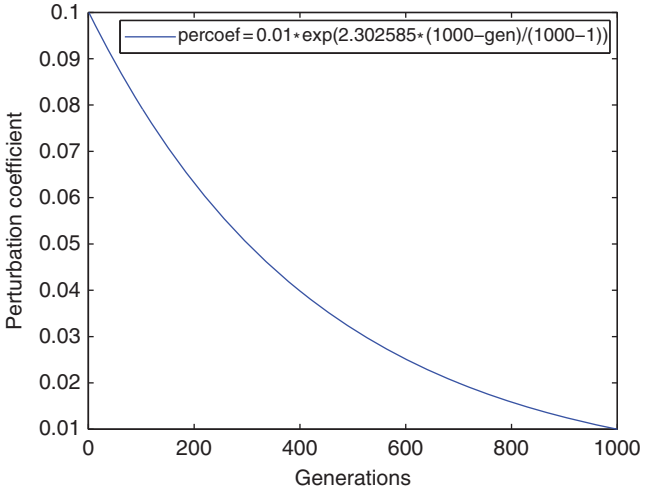

Figure 1. Perturbation coefficient decreasing with generation.

Table 1. Benchmarks for simulations.

Functions	Mathematical expression	Range of search	Initialization
Sphere function	$f_1(x) = \sum_{i=1}^{n} x_i^2$	$(-100,\ 100)^n$	$(50,\ 100)^n$
Rosenbrock function	$f_2(x) = \sum_{i=1}^{n} [100(x_{i+1} - x_i^2)^2 + (x_i - 1)^2]$	$(-100,\ 100)^n$	$(15,\ 30)^n$
Rastrigrin function	$f_3(x) = \sum_{i=1}^{n} [x_i^2 - 10\cos(2\pi x_i) + 10]$	$(-10,\ 10)^n$	$(2.56,\ 5.12)^n$
Griewank function	$f_4(x) = \frac{1}{4000}\sum_{i=1}^{n} x_i^2 - \prod_{i=1}^{n} \cos(\frac{x_i}{\sqrt{i}}) + 1$	$(-600,\ 600)^n$	$(300,\ 600)^n$
Schaffer's function	$f_5(x) = 0.5 - \frac{(\sin\sqrt{x^2+y^2})^2 - 0.5}{(1.0+0.001(x^2+y^2))^2}$	$(-100,\ 100)^2$	$(15, 30)^2$
Shifted sphere function	$f_6(x) = f\_bias + \sum_{i=1}^{n} (x_i - o_i)^2 f\_bias = -450$	$(-100, 100)^n$	$(-100, 100)^n$
Shifted Ackley function	$f_7(x) = 20 - 20\exp\left(-0.2\sqrt{\frac{1}{n}\sum_{i=1}^{n}(x_i - o_i)^2}\right) + e - \exp\left(\frac{1}{n}\sum_{i=1}^{n}\cos(2\pi(x_i - o_i))\right) + f\_bias$, $f\_bias = -140$	$(-32, 32)^n$	$(-32, 32)^n$

Notes: $o = [o_1, o_2, \ldots, o_n]$ – the shifted global optimum; *f_bias* – global optimal function value.

Compute p by Equation (18);
Update the positions of all particles according to Equation (25);
Evaluate all the particles $J[X_i(k)]$, $i = 1, 2, \ldots, M$ according to Equation (8)
Do perturbations to all particles according to Equation (27);
Re-evaluate all the particles $J[X_i^{per}(k)]$, $i = 1, 2, \ldots, M$ according to Equation (8);
Update *pbest* P and *gbest* P_g;
Update contraction–expansion coefficient according to Equation (26);
$k = k + 1$;
End while
Output *gbest* P_g.

4. Numerical tests for the improved QPSO with perturbation operator

4.1. *Benchmarks and parameters settings*

Seven well-known benchmarks were used to evaluate the performance of the proposed improved QPSO method with a perturbation operator (QPSO-PER), both in terms of the optimum solution and the rate of convergence to the optimum solution. These benchmark functions were widely used in evaluating performance of evolutionary methods [17–20,24–28]. All the functions are all minimization problems. Functions (f_1–f_5) have the global minimum at the origin or very close to the origin, while functions (f_6–f_7) have the global optimum at $o = [o_1, o_2, \ldots, o_n]$ and the global minimum at *f_bias*. All benchmark functions used are given in Table 1, which also shows the range of population initialization and the search scope for each function.

Simulations were carried out to observe the rate of convergence and the quality of the optimum solution of the proposed method introduced in this investigation in comparison with the original PSO, GA and simple QPSO. The neighbourhood of a particle is the whole population, which is named the global best model. All benchmarks with the exception of Schaffer's function were tested with dimensions 10, 20, and 30. For each function, 50 trials were carried out and the average optimal value and the standard deviations are presented. A different number of maximum generations ($G_{\max}$) is used according to the dimensionality of the problem under consideration. In this article, all empirical experiments were carried out with a population size of 30.

4.2. *Results from benchmark simulations*

The mean best values and standard deviation for 50 trials of each algorithm on each of the nine benchmark functions are listed in Table 2. The numerical results show that the improved QPSO-PER performed better on almost all the tested functions than the original PSO and simple QPSO.

The convergences (optimum solution over the iterations) of the original PSO, simple QPSO and the improved QPSO are shown in Figure 2. All the benchmarks except Schaffer's f_6 function are considered in 30 dimensions. In Figure 2(a)–(d), QPSO-PER works almost the same as or even worse than QPSO in the former stages, while due to the perturbation applied to the particles, the diversity of the population increases, so the particles can avoid becoming premature and escape from the local optima.

5. Numerical experiments of QPSO for solving the inverse source problems

In order to verify the efficiency and validity of the proposed methods and compare the performance of the original PSO, simple QPSO and improved QPSO to solve this inverse source problem, a typical example used by many researchers [1–6] is considered here:

$$c_{in}(t) = \exp\left[-\frac{(t-130)^2}{2\cdot 5^2}\right] + 0.3\exp\left[-\frac{(t-150)^2}{2\cdot 10^2}\right] + 0.5\exp\left[-\frac{(t-190)^2}{2\cdot 7^2}\right]. \tag{28}$$

We reconstructed the source history using measured concentration sampling between $t \in [0, 300]$ ($t_f = 300$), with $V = 1.0$ and $D = 1.0$. The time step is chosen as $\Delta t = 3.0$ and the mesh size is set as $\Delta x = 1.0$.

Figure 3 shows the source history, in which we can easily see that three peaks exist. This true release history is used to generate the contaminant concentration that is treated as the simulated measured concentration. Figure 4 shows the concentration distribution after 300 time units and the locations of the measurements.

In our numerical experiments, the parameters in original PSO are set, respectively, as $M = 50$, $D = 300/\Delta t = 300$, $V_{\max} = 1.2$, $c_1 = c_2 = 2.0$, $\omega_0 = 0.9$, $\omega_1 = 0.4$ and $k_{\max} = 2000$. In order to compare the results in the same condition, most of the parameters in simple QPSO, and the improved QPSO were set to be the same value as those in the original PSO.

To compare the results for situations involving random measurement errors, normal distribution uncorrelated errors with zero mean and constant standard deviation were

Table 2. Results for all the benchmarks.

Function	Dimension	G_{max}	Mean best value (standard deviation)		
			PSO	QPSO	QPSO-PER
f_1	10	1000	5.42E−23 (1.99E−22)	0.00 (0.00)	0.00 (0.00)
	20	2000	3.90E−19 (1.30E−18)	2.49E−42 (0.00)	1.40E−45 (0.00)
	30	3000	3.43E−15 (8.94E−15)	1.67E−34 (0.00)	8.41E−45 (0.00)
f_2	10	1000	56.80 (85.75)	30.55 (60.17)	21.86 (28.02)
	20	2000	113.03 (204.15)	55.41 (58.03)	42.10 (34.63)
	30	3000	152.36 (228.74)	65.93 (64.45)	41.75 (31.07)
f_3	10	1000	4.23 (2.11)	4.67 (2.59)	3.78 (1.97)
	20	2000	17.73 (4.34)	14.35 (4.23)	10.89 (3.43)
	30	3000	37.67 (9.73)	24.83 (6.74)	19.99 (5.62)
f_4	10	1000	9.12E−02 (3.79E−02)	4.96E−02 (4.09E−02)	3.36E−02 (3.28E−02)
	20	2000	2.40E−02 (1.62E−02)	1.76E−02 (1.61E−02)	1.53E−02 (2.45E−02)
	30	3000	1.80E−02 (1.95E−02)	9.68E−03 (1.29E−02)	4.93E−03 (8.53E−03)
f_5	2	1000	2.46E−03 (9.50E−09)	2.46E−03 (1.71E−08)	2.46E−03 (2.14E−10)
f_6	10	1000	−450+ 1.47E−22 (4.23E−20)	−450+ 3.19E−43 (2.20E−42)	−450+ 4.98E−43 (1.87E−43)
	20	2000	−450+ 2.12E−19 (1.16E−19)	−450+ 1.91E−34 (7.15E−34)	−450+ 1.85E−36 (3.80E−35)
	30	3000	−450+ 5.01E−16 (2.01E−15)	−450+ 7.37E−24 (2.17E−24)	−450+ 4.17E−32 (1.26E−33)
f_7	10	1000	−140+ 2.78E−06 (2.01E−12)	−140+ 2.78E−06 (4.33E−14)	−140+ 2.78E−06 (4.64E−15)
	20	2000	−140 + 0.40 (2.82)	−140 + 0.41 (2.87)	−140+ 2.78E−06 (8.31E−14)
	30	3000	−140 + 2.03 (6.10)	−140+ 2.78E−06 (1.01E−13)	−140+ 2.78E−06 (9.76E−14)

assumed. The simulated inexact measurement data $Y(x_i, t)$ can be expressed as

$$Y(x_i, t) = C_{exact}(x_i, t) + \varepsilon\delta_i C_{exact}(x_i, t), \tag{29}$$

where $C_{exact}(x_i, t)$ is the solution of the direct problem with the exact value of $C_{in}(t)$, ε is the noise level and δ_i is the ith standard normal random deviation of the noise which lies within the specified confidence bound. If we use a 99% confidence interval, $-2.576 < \delta_i < 2.576$.

First, numerical tests were performed to evaluate the effects of the sampling time (t_s) and location (x_s) on the solution of the inverse source problem. Details of the test runs are listed in Table 3. The results are presented in Figure 5 and Table 4. Obviously, samples obtained at many locations over a period of time produce more accurate results than other two types of sampling.

To analyse the effect of the regularization term on the solution of the inverse source history problem, two different scenarios were tested. The details are given in Table 5.

Figure 6 shows the reconstructed source history by QPSO, in which exact measurements without noise were used, first- and zeroth-order regularization terms were tested, the optimal regularization parameters obtained by the L-curve method are $\lambda = 6 \times 10^{-3}$. The compared results are given in Table 6. From the results, we can note that the first-order

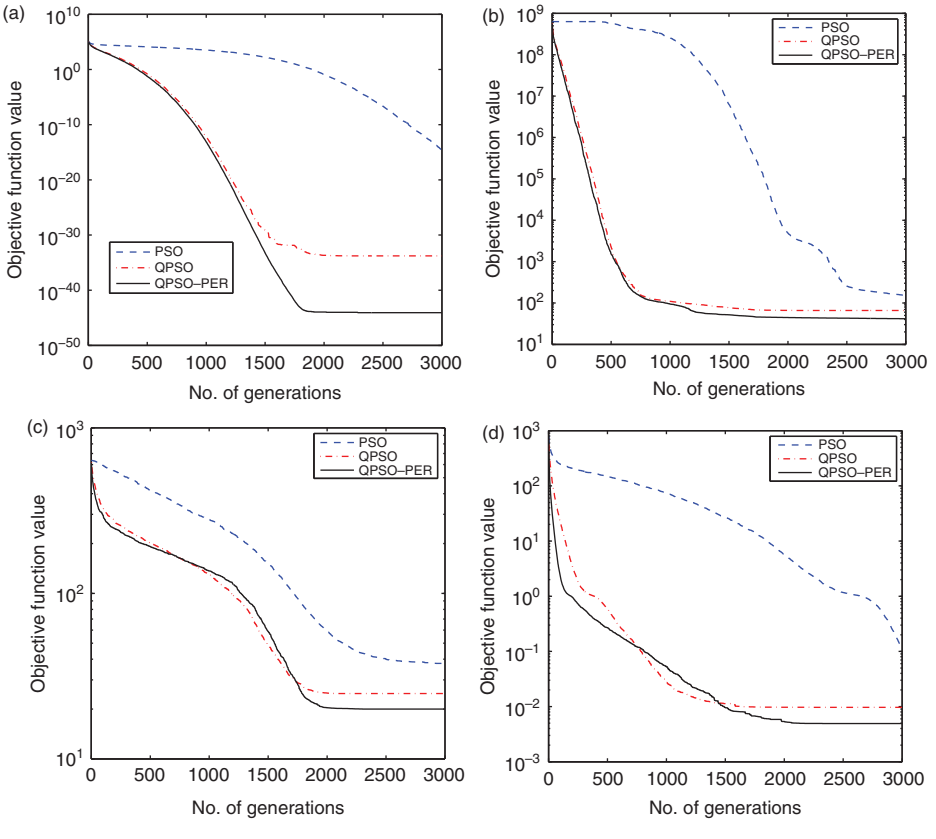

Figure 2. The comparison of convergence between the original PSO, simple QPSO, and QPSO-PER: (a) f_1 (sphere), (b) f_2 (Rosenbrock), (c) f_3 (Rastrigrin), (d) (Griewank), (e) f_6 (Schaffer), (f) (shifted sphere) and (g) (shifted Ackley).

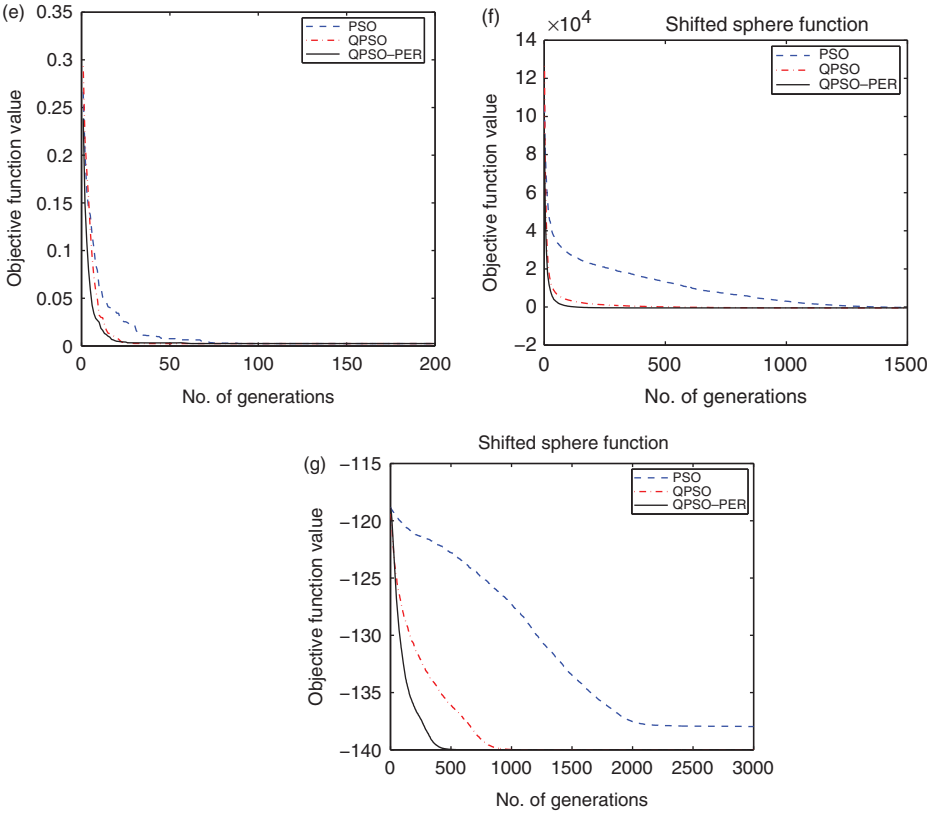

Figure 2. Continued.

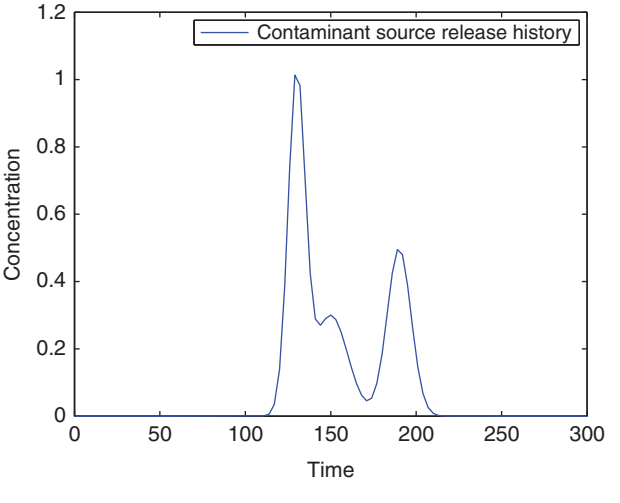

Figure 3. The time-varying contaminant release history.

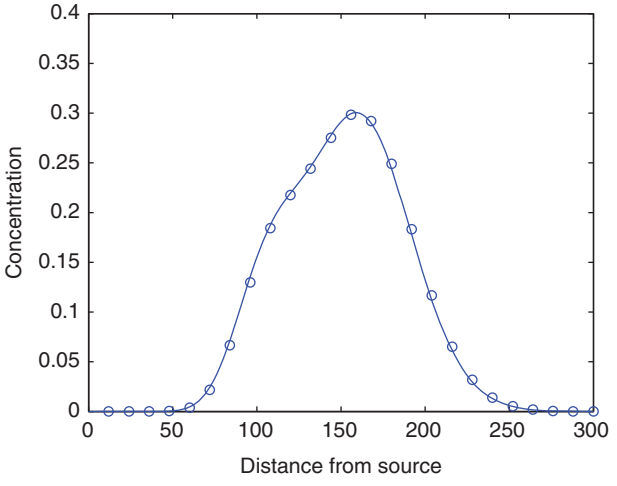

Figure 4. Contaminant plume after 300 time units, with measurement locations denoted by circles.

Table 3. Test scenarios for the analysis of the sampling time and location.

Run number	Sampling time	Sampling location
Run1	$t_s = t_f$	25 locations denoted in Figure 4
Run2	$t_s = \Delta t, 2\Delta t, \ldots, t_f$	$x_s = L/2$ (middle of the domain)
Run3	$t_s = \Delta t, 2\Delta t, \ldots, t_f$	25 locations denoted in Figure 4

regularization can deal with the non-smooth function effectively, while the zeroth-order regularization term cannot reduce the oscillatory feature of the input function. The most important thing to us is that the QPSO method can reconstruct the unknown source history effectively.

In order to verify the stability of the QPSO for solving the inverse source history problem, measured concentration with noise was used in scenarios of Run6 and Run7, and results are shown in Figure 7 and Table 7. It can be noted from the results that the QPSO method was able to reconstruct the source history almost accurately even though with noisy measured samples.

For performance comparison, PSO and GA were also adopted to solve the inverse source history problems, testing scenarios are listed in Table 8. We can note from (Table 9) and (Figures 8–9) that the reconstructed source history and performance obtained by the QPSO were much better than that from the PSO and GA. For the stability in particular, the QPSO was more robust in dealing with the noisy samplings than its competitors.

Finally, the improved QPSO with a perturbation operator was applied to reconstruct the contaminant source history, with the test scenarios listed in Table 10. The results are shown in Figure 10 and Table 11, from which we can observe that the improved QPSO with perturbation operator was able to estimate the unknown source history function much more accurately than that obtained by other methods. The convergence of the

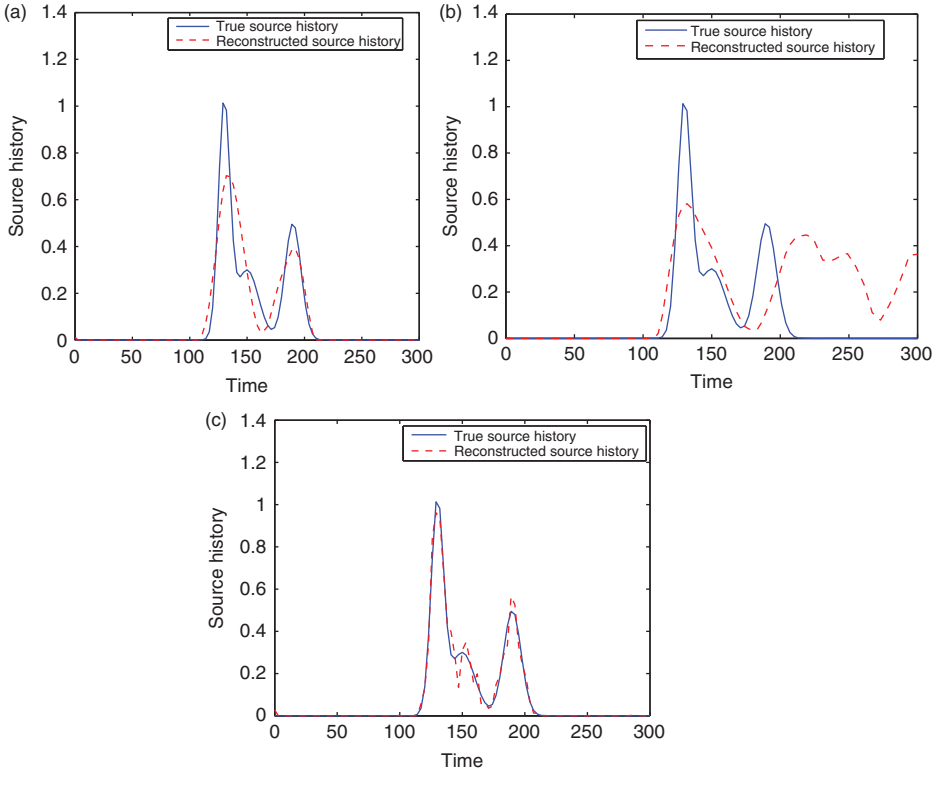

Figure 5. Results of sampling time and location verification by simple QPSO in Run1–Run3. Reconstructed source history with data in: (a) Run1, (b) Run2 and (c) Run3.

Table 4. Results of analysis of the sampling time and location.

Run number	Average error	Residual norm
Run1	7.96E−03	5.20E−06
Run2	2.12E−02	1.00E−04
Run3	2.95E−03	3.38E−04

Table 5. Test scenarios for the analysis of the regularization.

Run number	Regularization order	Noise level (ε)
Run4	First order	0
Run5	Zeroth order	0
Run6	First order	0.05
Run7	First order	0.2

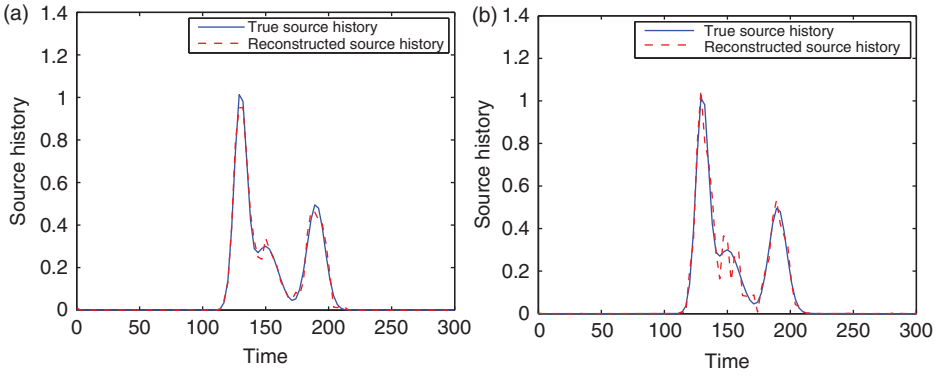

Figure 6. Results of regularization term verification by simple QPSO in Run4 and Run5, with noise-free measurements. Reconstructed source history with: (a) Run4 and (b) Run5.

Table 6. Results of the analysis of the regularization.

Run number	Average error	Residual norm
Run4	1.81E−03	2.03E−04
Run5	3.49E−03	3.12E−04

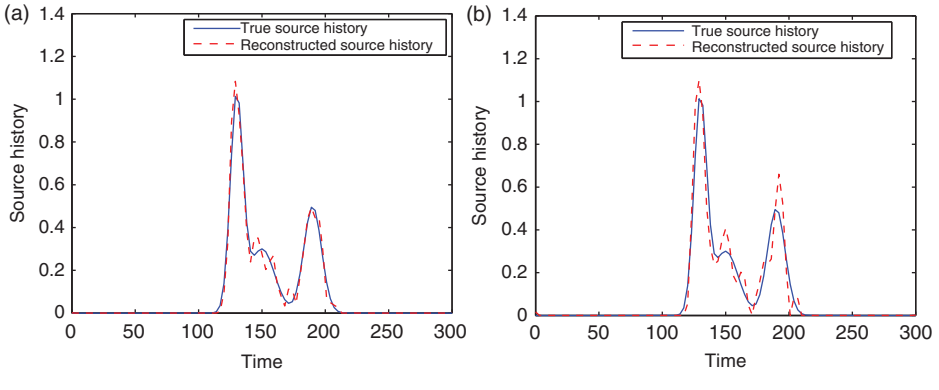

Figure 7. Results of stability verification for simple QPSO in Run6 and Run7 with noisy measurements. Reconstructed source history using: (a) Run6 and (b) Run7.

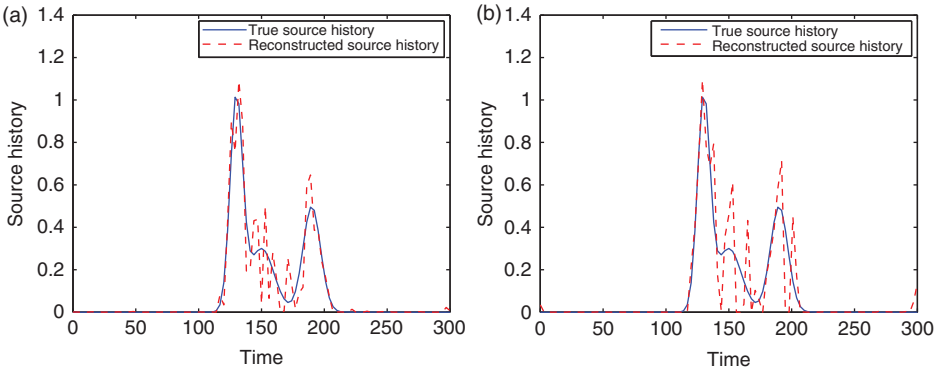

Figure 8. Reconstructed source history by original PSO in: (a) Run8 and (b) Run9.

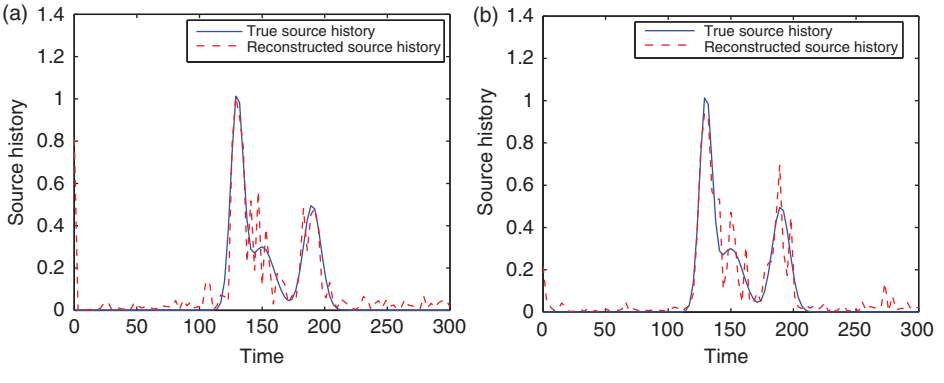

Figure 9. Reconstructed source history by GA in: (a) Run10 and (b) Run11.

Table 7. Results of the analysis of noisy measurements.

Run number	Average error	Residual norm
Run6	2.94E−03	7.66E−02
Run7	2.07E−03	0.29

Table 8. Testing scenarios by the original PSO and GA.

Run number	Methods	Noise level (ε)
Run8	PSO	0.0
Run9	PSO	0.1
Run10	GA	0.0
Run11	GA	0.1

Table 9. Results of the original PSO and GA for solving the inverse source history problem.

Run number	Average error	Residual norm
Run8	7.59E−03	2.58E−03
Run9	1.02E−02	0.31
Run10	1.10E−02	0.32
Run11	7.10E−03	0.46

Table 10. Testing scenarios by the improved QPSO (QPSO-PER).

Run number	Methods	Noise level (ε)
Run12	QPSO-PER	0.0
Run13	QPSO-PER	0.1

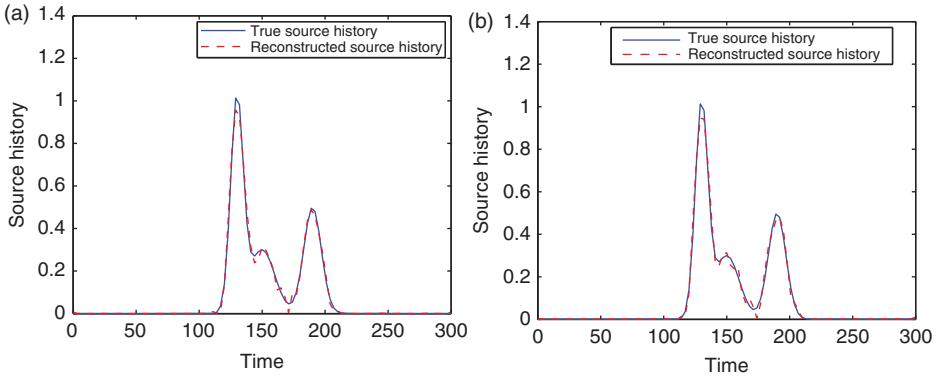

Figure 10. Reconstructed source history by QPSO-PER in: (a) Run12 and (b) Run13.

Table 11. Results of QPSO-PER for solving the inverse source problems.

Run number	Average error	Residual norm
Run12	1.59E−03	1.89E−04
Run13	3.64E−03	0.28

methods used in this article for solving the inverse source history problems is shown in Figure 11, which shows the better convergence properties of QPSO and QPSO-PER.

6. Conclusions

An improved version of the QPSO-PER is proposed in this article, with the test results of the benchmark functions demonstrating the validity and efficiency of the proposed

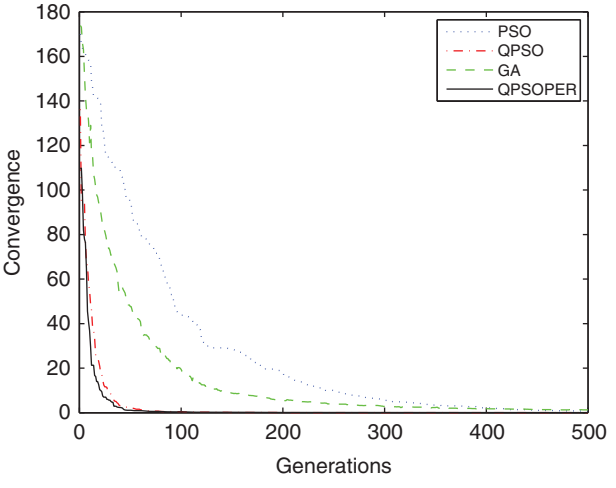

Figure 11. Convergence of the methods used for solving the inverse source history problems.

improved method. Both the optimum solution and the convergence rate of QPSO-PER are better than other methods, or have competitive performance. Because of the perturbation operator introduced in the QPSO-PER, particles can escape from the local optimum and avoid being premature. After that, the proposed methods were used to solve the inverse contaminant source history problems, in which no prior information about the functional form is available and many peaks exist in the function. The numerical experimental results suggest that these methods were all able to converge to the optimal or sub-optimal solutions. The QPSO-PER was more robust than other methods in dealing with the noisy samplings.

According to the existing literatures, in which other gradient-based deterministic methods (MRE, TR) are used to reconstruct the unknown source history, the great advantages of the stochastic methods, such as QPSO, are that they do not need to compute the complicated gradient of the objective function, and can guarantee the convergence to the global optimum.

Considering the difficulty of computing the Lagrange multiplier in the MRE method, our future study will focus on proposing a hybrid method to combine the stochastic and MRE methods, and then applying it to solve the more complicated inverse problems.

Acknowledgements

This study is supported by 'the Fundamental Research Funds for the Central Universities' (project no. JUSRP21012), the innovative research team project of Jiangnan University (project no. JNIRT0702) and the National Natural Science Foundation of China (project no. 60973094).

References

[1] P. Sidauruk, *Parameter determination for multi-layered aquifer and groundwater contaminant transport*, Ph.D. diss., University of Delaware, 1996.

[2] S.M. Gorelick, B. Evans, and I. Remson, *Identifying sources of groundwater pollution: An optimization approach*, Water Resources Res. 19 (1983), pp. 779–790.
[3] B.J. Wagner, *Simultaneous parameter estimation and contaminant source characterization for coupled groundwater flow and contaminant transport modeling*, J. Hydrol. 135 (1992), pp. 275–300.
[4] S. Zou and A. Parr, *Estimation of dispersion parameters for two dimensional plumes*, Ground Water 31 (1993), pp. 389–392.
[5] H.T. Skaggs and Z.J. Kabala, *Recovering the release history of a groundwater contaminant*, Water Resources Res. 30 (1994), pp. 71–79.
[6] H.T. Skaggs and Z.J. Kabala, *Limitations in recovering the history of a groundwater contaminant plume*, J. Contam. Hydrol. 33 (1998), pp. 347–359.
[7] H.T. Skaggs and Z.J. Kabala, *Recovering the history of a groundwater contaminant plume: Method of quasi-reversibility*, Water Resources Res. 31 (1995), pp. 2669–2673.
[8] A.D. Woodbury and T.J. Ulrych, *Minimum relative entropy inversion: Theory and application to recovering the release history of a groundwater contaminant*, Water Resources Res. 32 (1996), pp. 2671–2681.
[9] A.D. Woodbury, E. Sudicky, T.J. Ulrych, and R. Ludwig, *Three-dimensional plume source reconstruction using minimum relative entropy inversion*, J. Contam. Hydrol. 32 (1998), pp. 131–158.
[10] M.F. Snodgrass and P.K. Kitanidis, *A geostatistical approach to contaminant source identification*, Water Resources Res. 33 (1997), pp. 537–546.
[11] N.Z. Sun, *Inverse Problems in Groundwater Modeling*, Kluwer, Dordrecht, The Netherlands, 1994.
[12] O.M. Alifanov, *Inverse Heat Transfer Problems*, Springer, Berlin, 1994.
[13] T.H. Nguyen, *Optimization Approach to the* Inverse *Convection Problem*, Proceedings of the International Workshop on Inverse Problems, Ho Chi Minh City, Vietnam, 1995.
[14] R. Fletcher, *Practical Methods of Optimization*, Wiley, New York, 1987.
[15] C. Liu and W.P. Ball, *Application of inverse methods to contaminant source identification from aquitard diffusion profiles at Dover AFB, Delaware*, Water Resources Res. 35 (1999), pp. 1975–1985.
[16] T.V. Bharat, P.V. Sivapullaiah, and M.M. Allam, *Accurate Parameter Estimation of Contaminant Transport Inverse Problem using Particle Swarm Optimization*, IEEE Swarm Intelligence Symposium, St Louis, MO, September 21–23, 2008.
[17] J. Sun, B. Feng, and W.B. Xu, *Particle Swarm Optimization with Particles Having Quantum Behavior*, Proceedings of the Congress on Evolutionary Computation, Oregon, Portland, 2004.
[18] J. Sun, W.B. Xu, and B. Feng, *A Global Search Strategy of Quantum-behaved Particle Swarm Optimization*, Proceedings of IEEE International Conference on Cybernetics and Intelligent Systems, Singapore, 2004.
[19] J. Sun and W.B. Xu, *Adaptive Parameter Control for Quantum-behaved Particle Swarm Optimization on Individual Level*, Proceedings of IEEE International Conference on Systems, Man and Cybernetics, Hawaii, 2005.
[20] J. Kennedy and R.C. Eberhart, *Particle swarm optimization*, Proc. IEEE Int. Conf. Neural Networks 4 (1995), pp. 1942–1948.
[21] A.N. Tikhonov and V.Y. Arsenin, *Solution of Ill-Posed Problems*, Winston, Washington, DC, 1977.
[22] P.C. Hansen and D.P. O'Leary, *The use of the L-curve in the regularization of discrete ill-posed problems*, SIAM J. Sci. Comput. 14 (1993), pp. 1487–1503.
[23] P.C. Hansen, *Analysis of discrete ill-posed problems by means of the L-curve*, SIAM Rev. 34 (1992), pp. 561–580.
[24] M. Raudensky, J. Horsky, J. Krejsa, and L. Slama, *Usage of artificial intelligence methods in inverse problems for estimation of material parameters*, Int. J. Numer. Methods Heat Fluid Flow 6 (1996), pp. 19–29.

[25] J. Kennedy and R.C. Eberhart, *Swarm Intelligence*, *Morgan Kaufmann Series in Evolutionary Computation*, Morgan Kaufmann, San Francisco, CA, 2001.
[26] M. Clerc, *The swarm and queen: Towards a Deterministic and Adaptive Particle Swarm Optimization*, Proceedings of the IEEE Congress on Evolutionary Computation, Washington, DC, 1999.
[27] F. Van den Bergh, *An analysis of particle swarm optimizers*, Ph.D. diss., University of Pretoria, South Africa, 2001.
[28] M. Clerc and J. Kennedy, *The particle swarm: Explosion, stability, and convergence in a multi-dimensional complex space*, IEEE Trans. Evol. Comput. 6 (2002), pp. 58–73.
[29] H.X. Long, J. Sun, X.G. Wang, C-H. Lai, and W.B. Xu, *Using selection to improve quantum-behaved particle swarm optimization*, Int. J. Innovative Comput. Appl. 2 (2009), pp. 100–114.
[30] J. Sun, W.B. Xu, and W. Fang, *A diversity-guided quantum-behaved particle swarm optimization algorithm*, Simulated Evolution and Learning 4247 (2006), pp. 497–504.
[31] J. Sun, W.B. Xu, and W. Fang, *Quantum-behaved particle swarm optimization algorithm with controlled diversity*, ICCS, 3993 (2006), pp. 847–854.
[32] T.V. Bharat, *Novel agitated particle swarm algorithms for function optimization*. J. Comput. Intell (submitted).
[33] T.V. Bharat, V.S. Puvvadi, and M.A. Mehter, *Swarm intelligence based inverse model for characterization of groundwater contaminant source*, Electron. J. Geotech. Eng. 14 (2006), p. 14, Available at http://www.ejge.com/2009/Ppr0850/Ppr0850.pdf.
[34] J. Liu, J. Sun, and W.B. Xu, *Quantum-behaved particle swarm optimization with adaptive mutation operator*, ICNC, 4221 (2006), pp. 959–967.